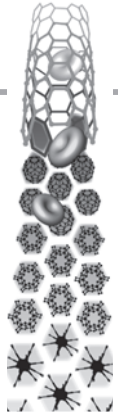

Carbon nanotube-mediated wireless cell permeabilization: drug and gene uptake

Aim: This work aims to exploit the 'antenna' properties of multiwalled carbon nanotubes (MWCNTs). They can be used to induce cell permeabilization in order to transfer drugs (normally impermeable to cell membranes) both in *in vitro* and *in vivo* models. **Material & Methods:** The performance of the MWCNTs as receiver antenna was modeled by finite element modeling. Once the appropriate field has been identified, the antenna properties of MWCNTs were investigated in sequential experiments involving immortalized fibroblast cell line (drug model: doxorubicin chemothererapeutic agent) and living mice (drug model: *bcl-2* antiapoptotic gene) following stereotactic injection in the cerebral motor cortex. **Results:** Finite element modeling analysis predicts that our MWCNTs irradiated in the radiofrequency field resemble thin-wire dipole antennas. *In vitro* experiments confirmed that combination of MWCNTs and electromagnetic field treatment dramatically favors intracellular drug uptake and, most importantly, drug nuclear localization. Finally, the brain of each irradiated animal exhibits a significantly higher number of transfected cells compared with the appropriate controls. **Conclusion:** This wireless application has the potential for MWCNT-based intracellular drug delivery and electro-stimulation therapies.

KEYWORDS: brain transfection ■ carbon nanotubes ■ cell permeabilization ■ electromagnetic field

Vittoria Raffa[1‡], Lisa Gherardini[2‡], Orazio Vittorio[1‡], Giuseppe Bardi[3], Afshin Ziaei[4], Tommaso Pizzorusso[2], Cristina Riggio[1], Stephanos Nitodas[5], Theodoros Karachalios[5], Khuloud T Al-Jamal[6], Kostas Kostarelos[6], Mario Costa*[2,7] & Alfred Cuschieri[1]

[1]Medical Science Lab, Scuola Superiore Sant'Anna, Pisa, 56127, Italy
[2]Neuroscience Institute, CNR, Pisa, 56127, Italy
[3]Center for Nanotechnology Innovation @ NEST, Istituto Italiano di Tecnologia, Pisa, Italy
[4]Thales Research & Technology France, Palaiseau cedex, F-91767, France
[5]Nanothinx S.A. Rio-Patras, 26500, Greece
[6]The School of Pharmacy, University of London, London, WC1N 1AX, UK
[7]Laboratory of Neurobiology, Scuola Normale Superiore, Pisa, Italy
**Author for correspondence: costa@in.cnr.it*
‡Authors contributed equally

Carbon nanotubes (CNTs) are seamless rolled up cylinders of graphene sheets, exhibiting many unique physical, mechanical and chemical properties, that have attracted considerable scientific interest over the past decade [1]. CNTs can be classified in two general categories based on their structure: single-walled (SWCNT), which consist of one layer of cylinder graphene and multiwalled (MWCNT), which contain several concentric graphene sheets. The hydrophobicity of CNTs has for a long time been a major limitation for their biological use. This problem has been resolved by significant progress in chemical coating that permits their dispersion in aqueous solutions [2] and has made their translation as biomaterials possible for a variety of medical applications [3,4]. The progress in CNT solubilization and their consequent biological application unveiled the problem of the intrinsic toxicity of these nanomaterials on cells and tissue. The discrepancy observed in toxicity effects of nanotubes might reflect the lack of proper characterization (morphology, purity, metal content and carbon soot) of CNTs, which are often produced by various sources [5]. Many groups observed that toxic effects induced by CNTs were the result of high content of residual metal catalyst and contaminants present in the unrefined CNTs [6,7]. Another critical features of the CNTs is their length; it has been reported that CNTs >10–15 µm long can induce the formation of granulomas due to 'frustrated phagocytosis' similar to those caused by asbestos fibers when implanted intraperitonealy in mice [8]. It is equally important to use valid and reliable *in vitro* tests for cell viability measurement following exposure to CNTs. Indeed, some of the data reported in the literature were obtained with various cell viability assays which incorporate reagents that have since been shown to interact directly with the CNTs, and thus provide spurious and unreliable estimates of cell viability [9,10]. For this reason, the biological compatibility of the CNTs employed in the present study was carefully established by our group in previous works by use of appropriate biological assays [11–13]. More specifically, eukaryotic cell lines, cultured with 5 µg ml^{-1} of nanotubes, showed negligible loss of cell viability (<5%, upon 3 weeks of continued propagation in the presence of the nanotubes), and no apoptosis or induction of reactive oxidative stress. Toxicity studies on primary cell culture confirmed that 5 µg ml^{-1} MWCNTs did not induce neuron apoptosis *in vitro*. Additionally, we demonstrated that MWCNTs can be injected in the mouse cerebral cortex without causing degeneration of the neurons surrounding the site of injection.

The superior mechanical strength and chemical inertness render CNTs ideal for applications

future medicine part of fsg

in tissue engineering and myocardial regeneration [14]. In addition to these structural characteristics, the electrical properties of the nanotubes are potentially useful in stimulating electrical activity, and this application is being explored for its use in neuroprosthetics [15–19]. Another important feature of CNTs is their ability to cross cell membranes by endocytosis or diffusion [20], which underpins their use as vectors for the delivery of drugs, peptides and genes [21–25]. This key feature also takes into account the potential biological risk related to the biomedical use of CNTs. We investigated these issues in a previous work. We demonstrated that the cellular uptake of MWCNTs dispersed in Pluronic F127 proceeds via an energy independent pathway (i.e., diffusion) and clearly depends on the nanotube length. Experimental results showed that MWCNTs with length <1 µm were easily accumulated within cells while the uptake of 1 µm MWCNTs was negligible [26].

The key advantage for the use of CNTs in medicine over other nanoparticles, such as polymeric nanoparticles, lies in their unique and synergistic combination of electric, optical and chemical properties. This accounts for the significant potential of CNTs as novel vectors/carriers for targeted drug delivery systems, ushering in newer forms of more effective drug therapy. Despite the considerable research in this field thus far, a technology that combines the chemical and physical properties of CNTs for *in vivo* gene and drug therapy is not yet available, although published reports have demonstrated the effective use of the strong near-infrared absorbance of SWCNTs for selective thermal ablation of cancer cells [27]. Similarly, thermal destruction of malignant cells has been reported in animal models based on heat release from SWCNTs in a radiofrequency (RF) field [28]. Interestingly, MWCNT-mediated electroporation has been proposed by exploiting the field emission properties of MWCNTs for introducing gold nanoparticles in Gram-negative bacteria by microwave irradiation [29]. Moreover, we have successfully exploited the dielectric properties of MWCNTs for *in vitro* intracellular delivery of small molecules at low voltages [30].

The novelty of the present work lies in demonstrating, for the first time, that the 'antenna' properties of MWCNTs can be used to induce remote wireless cell permeabilization by microwave energy. This has been proven by both *in vitro* and *in vivo* experiments. In order to design the most effective experimental set-up, we initially modeled the features of a nanotube antenna in a water environment. A robust theoretical model was built that predicted the appropriate electromagnetic field wavelength and frequency. The output of the model was then successfully applied in experiments involving immortalized fibroblast cell line and living mice.

Experimental

Method of evaluating cell viability of MWCNTs

Multiwalled CNTs were supplied from Nanothinx S.A. (Rio Patras, Greece). Production method was by catalytic chemical vapor deposition of hydrocarbon sources on substrates of metal oxides impregnated with metal catalysts. We employed MWCNTs with a high degree of purity (97.06%), low amorphous carbon (<1%) and 2.94% metal impurities (Al and Fe, with the ratio Fe/Al being 7 ± 1 w/w) [26–31].Aqueous solutions of MWCNTs were made with Pluronic F127 (polyoxyethylene-polyoxypropylene block copolymer, supplied by Sigma, St. Louis, MO, USA) with the aid of magnetic stirring and sonication [32].

Cell cultures

Mouse fibroblasts NIH-3T3 (CCL-1658, purchased from ATCC), were cultured in Dulbecco's modified Eagle's medium with 10% fetal bovine calf serum, 100 IU ml^{-1} penicillin, 100 µg ml^{-1} streptomycin and 2 mM L-glutamine. Cells were maintained at 37°C in a saturated humidity atmosphere containing 95% air/5% CO_2.

Cell viability was monitored by colony assay. The colony assay was performed by plating 5000 cells for a Petri dish. All the assays were performed in triplicate. After 7 days from the seeding, the cells were washed, fixed, colored with cresyl violet and counted.

Time-lapse imaging

Time-lapse imaging experiments were performed on a Leica TCS NT confocal microscope with an oil immersion lens (Leica HCX APO 40×, NA 1.25). Doxorubicin (Dox) hydrochloride was purchased from Sigma-Aldrich. Quantification of fluorescence was performed on Leica platform software. Data plotting and statistical testing has been performed with the Origin 7 package.

Electromagnetic field irradiation

Irradiation was performed with a microwave signal. The set-up used to irradiate the sample is formed by a synthesizer Agilent 83623B and a microwave amplifier Microwave Power C0812–46. NIH-3T3 cells and animals were irradiated

with a little horn working in the 8–12 GHz frequency band (SUPPLEMENTARY INFORMATION 2, see online www.futuremedicine.com/doi/suppl/10.2217/nnm.11.62).

Intracerebral injections

Animals were used in accordance with protocols approved by the Italian Ministry for Scientific Research (document number 129/2000-A, issued on 13 December 2000). The document is a ministerial decree and The Institutional Animal Care and Use Committee (IACUC) approval. Mice were anesthetized with avertin (0.5 ml/100 g). Anesthetized mice were placed on a stereotactic platform and the scalp incised to expose the cranium. A small hole was drilled in the skull above the primary motor cortex (M1). 1 µl mixture suspension was injected 700 µm deep into the cortex by means of a manual pump equipped with a glass capillary. Plasmidic DNA alone or mixed with MWCNTs (ratio CNT/DNA 5:1 w/w), was injected stereotactically into the primary motor cortex (M1) of mice. In view of future possible applications in human CNS diseases (e.g., cerebrovascular stroke), we used a plasmidic expression vector carrying human *Bcl-2*, a well-characterized antiapoptotic gene, [33]. The plasmid encoding the *Bcl-2* gene was injected in the left cerebral hemisphere (control) while a mixture of plasmid and MWCNTs was injected in the contra-lateral hemisphere (test). Following closure of the scalp wound, the animal was placed in front of the electromagnetic sources, exposed to the appropriate treatment and allowed to recover. All these animals were sacrificed at 48 h after treatment and perfused with a solution of 4% paraformaldehyde.

Finite element method modeling

The model of the nanoantenna was performed by using a 3D electromagnetic simulation tool named high frequency simulation software (HFSS), by Ansoft Corporation. HFSS is a software that utilizes a 3D full-wave finite element method (FEM) to compute the electrical behavior of high-frequency and high-speed components. HFSS enables the extraction of the parasitic parameters (S, Y and Z), to visualize 3D electromagnetic fields (near and far field), to generate broadband SPICE models, and to optimize design performance. It accurately characterizes the electrical performance of components and effectively evaluates signal quality, including transmission path losses, reflection loss due to impedance mismatches, parasitic coupling and radiation. The performance of the MWCNTs as a receiver antenna was modeled in water (as the main constituent of the body). For the scope of this work, the refractive index of pure water can be considered not significantly different from that of a biological sample [34,35].

A HFSS tool was also used to simulate the penetration of the electric field inside the mouse brain. The mouse head was placed at the end of the horn. In this model the head was represented as consisting of three concentric spheres: an inner sphere (5 mm diameter) representing the brain (permittivity: 40; conductivity: 7 S/m), the central hollow sphere (inner diameter: 5 mm; thickness: 1 mm; permittivity: 14; conductivity: 3 S/m) representing the skull and the outer hollow sphere (inner diameter: 6 mm; thickness: 0.5 mm; permittivity: 32; conductivity: 7 S/m) representing the skin [36].

Results & discussion

Modeling a nanotube-like antenna

As the effectiveness of the MWCNT as an antenna strictly depends on its morphology, in the present study the nanotube morphology was carefully characterized by electron microscopy. The nanotubes used had diameters ranging between 19 and 40 nm, consisted of 20–42 layers (FIGURE 1A) and were 1 ± 0.5 µm in length. The metal impurities were enmeshed at the nanotube tip (FIGURE 1C). The main parameters influencing the antenna behavior are the diameter and the length. The diameter and the length distributions are Gaussian and present a peak. The simulations were run by considering a tube of 1 µm in

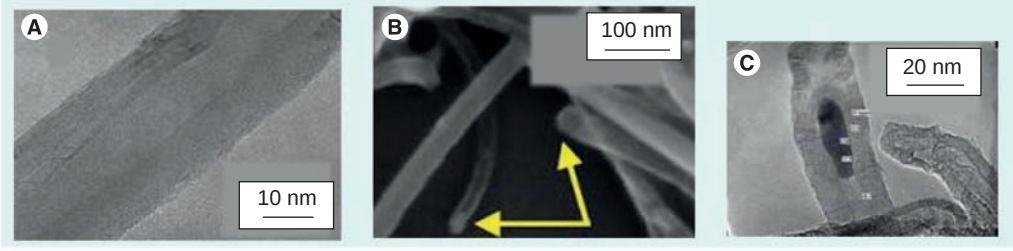

Figure 1. (A) Nanotube layers; (B) single nanotubes and (C) a nanotube entrapping a metal particle in the tip.

length and 25 nm in diameter (corresponding to the peaks). In this study, the resonator is a wire (of nanometric dimensions) excited by an electromagnetic signal that resonates at a specific frequency and creates an electromagnetic field of the same frequency in the surrounding space. Specifically, we used HFSS to draw a 3D model of the nanoantenna and set an excitation at the lower end, orthogonally to the wire antenna direction. After the simulation, we used the calculated electric field to visualize the radiation pattern, the return loss matching, the antenna gain, the directivity, the input impedance and the bandwidth of an antenna. We decided that a reasonable value for defining the bandwidth of the antenna would be for frequency whose return match is over 3 dB. The output of the simulation is provided in Figure 2. Finite element modeling based on the antenna theorem predicted that MWCNT dipole antennas resemble thin-wire dipole antennas for electromagnetic wave propagation at, or near, the free-space velocity of light. Interestingly, in agreement with our model, a recent work measured the antenna properties of MWCNTs irradiated in the RF field [37]. On the basis of prediction from this model, we used microwave radiation (3 cm) at 10 GHz frequency (additional information provided in Supplementary Information 1).

In vitro cell line experiments

CNT-mediated permeabilization was first confirmed on a mouse fibroblast cell line NIH-3T3. In order to acquire a real-time measure of the effect of electromagnetic field (EMF) and MWCNTs on cell permeabilization and intracellular drug concentration, we monitored the uptake of Dox, a fluorescent cytostatic drug used as the first-choice therapy in many malignancies. Dox exerts its effects by intercalating DNA and it is used extensively in biological research due to its intrinsic fluorescence [38]. Dox was added to the cell culture medium at a concentration of 100 µM. Dynamic imaging then enabled us

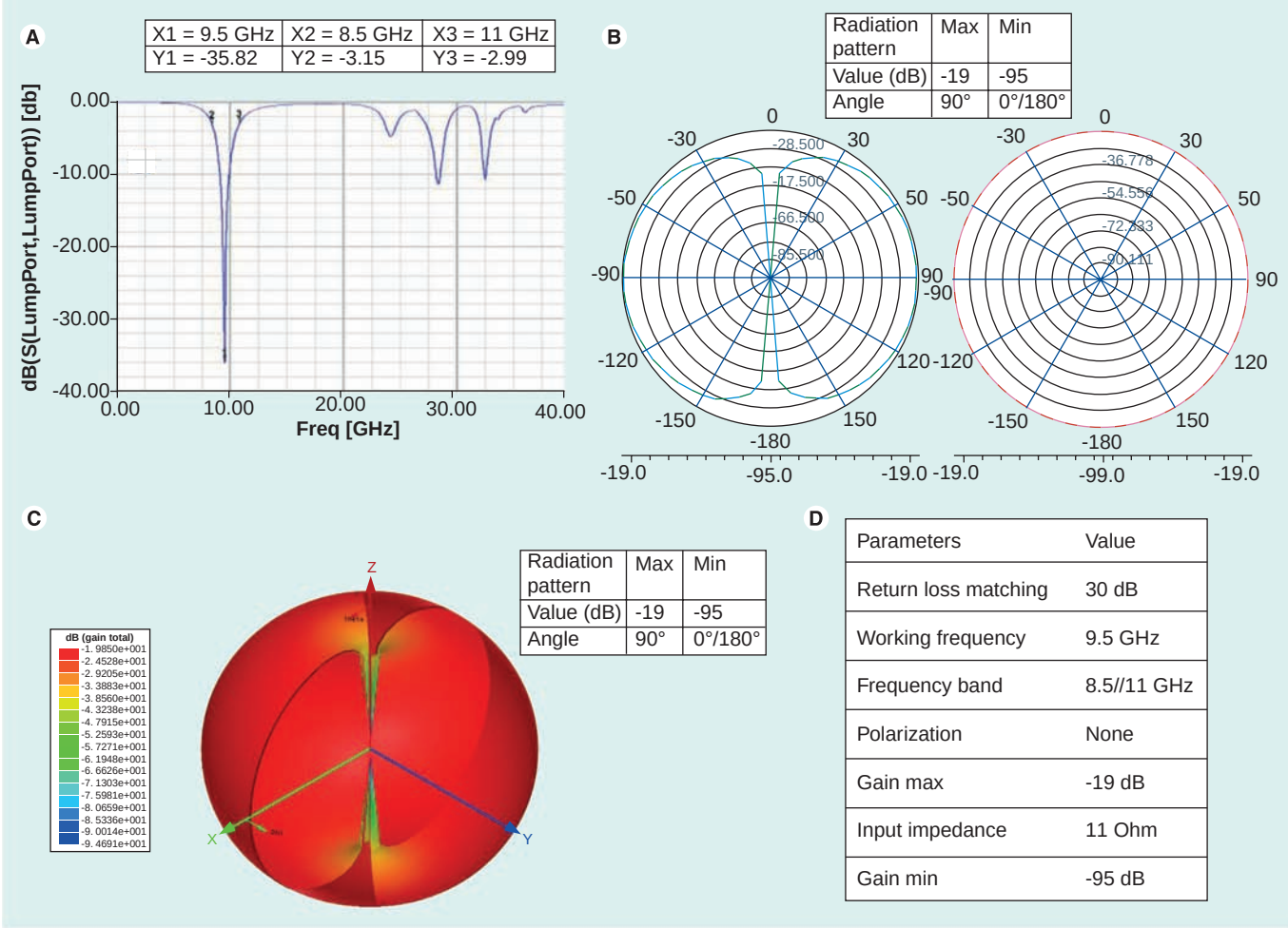

Figure 2. Finite element modeling of the nanotube antenna. (A) Return loss matching; **(B)** radiation pattern; **(C)** antenna gain; and **(D)** summary of antenna features.

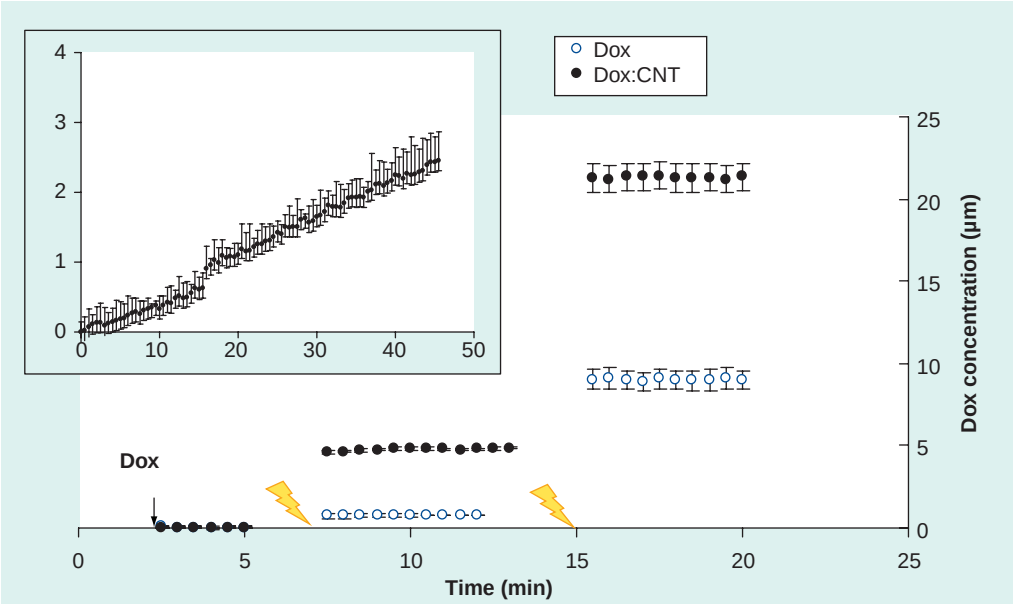

Figure 3. Time-lapse imaging of NIH-3T3 in the presence of doxorubicin 100 µM (white circle) and doxorubicin 100 µM:CNT 10 µg/ml (black circle). Normally growing NIH-3T3 cells were recorded initially to determine the background; at 2 min, cells were treated with Dox; at 7 min, the EMF field is applied (5 W, 10 s); at 15 min, the EMF field is applied again (5 W, 20 s). Inset: time-lapse imaging of NIH-3T3 in the presence of Dox 100 µM alone.
CNT: Carbon nanotube; Dox: Doxorubicin;

to visualize and quantify both Dox uptake and intracellular distribution [39,40]. In physiological conditions, Dox penetrates normally by passive mechanism of cellular uptake [41] with a slow internalization rate. Specifically, we estimated that the internalization dynamic of Dox alone (i.e., in absence of both CNTs and EMF) is linear up to 60 min with a kinetic constant of 1.5 ng $ml^{-1}s^{-1}$ (see inset of Figure 3). In the absence of CNTs or EMF, the intracellular concentration of Dox reached a maximum of 2.5 µM after 1 h of continuous incubation (Figure 3A)

Time-lapse recording showed that application of an incident power of 5 W for 10 s induced a sudden influx of Dox, reaching an intracellular concentration of up to 1 µM. Applying the same experimental conditions, but in the presence of MWCNTs, the Dox intracellular concentration rose dramatically to 6 µM. Notably, Dox influx was more pronounced at the time of the second EMF application, when a stronger energy dose (5 W, 20 s) was administered to the same cell cultures. Dox intracellular concentration reached 9 µM in the absence of MWCNTs and 21 µM in the presence of MWCNTs.

On examining the intracellular distribution of Dox we observed that the treatment with EMF and MWCNTs resulted in a distinctive nuclear and cytoplasmic localization of Dox. To quantify Dox distribution, we calculated the nuclear/cytoplasmic (N/C) ratio of Dox fluorescence intensity. We observed that when cells were treated with Dox and Dox:CNT without EMF, the drug accumulated mainly in the cytoplasm ($N/C < 1$). Conversely, application of EMF to cell culture alone, or in the presence of MWCNTs, coincides with a rapid step discontinuity in intracellular Dox concentration (Figure 3). Moreover, under EMF alone the intracellular drug distribution was homogeneous ($N/C \approx 1$), whereas with EMF in the presence of MWCNTs, the Dox accumulated preferentially in the nucleus ($N/C \approx 1.2$). The preferential nuclear localization is a crucial consideration for the cytotoxic action of drugs such as doxorubicin that interact directly with the nuclear DNA. Indeed, these findings suggest that the simultaneous use of CNT and EMF could be a useful tool to enhance the probability of Dox to accumulate in the nucleus and to exert its anticancer effect at lower dosage and limit the dangerous side effects.

In conclusion, these data indicate that the application of the EMF improves drug uptake and the phenomenon is strongly enhanced in the presence of CNTs. Moreover, the combination of CNT and EMF treatment dramatically favors nuclear localization of the drug (Figure 4). We investigated if the application of the electromagnetic field and consequent temperature modification could result in membrane breakdown or intracellular damages. The temperature profile was monitored with a k-thermocouple (sensitivity

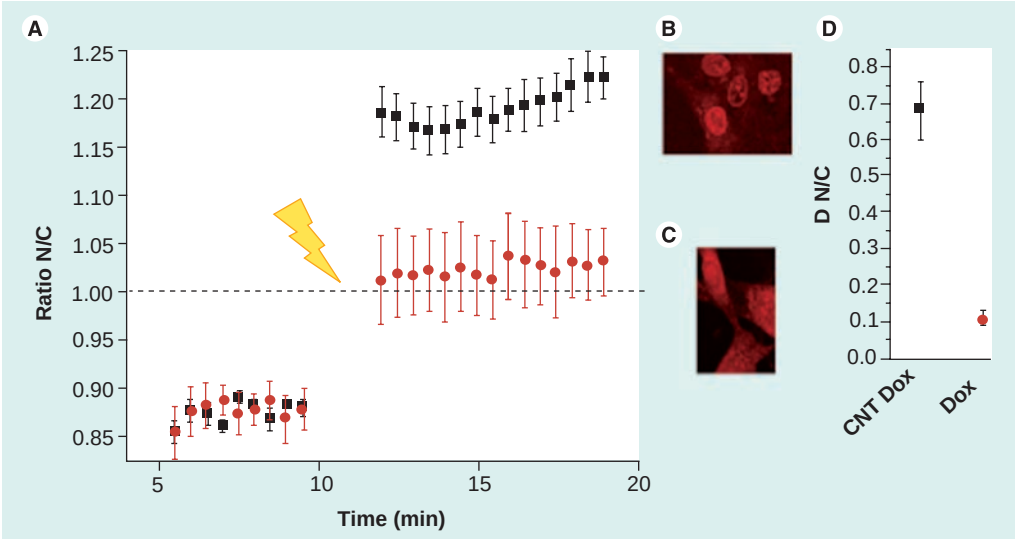

Figure 4. Time-lapse imaging of NIH-3T3 in the presence of doxorubicin 100 µM (red circles) and doxorubicin 100 µM:CNT 10 µg ml^{-1} (black squares). (A) Plot of the N/C ratio indicating the accumulation of Dox in cells before the electromagnetic field (EMF) application and following the application of EMF (flash); n = 8. **(B)** Fluorescence image of Dox distribution in the presence of the CNTs after application of the EMF. **(C)** Dox distribution in NIH-3T3 after application of EMF without CNTs. **(D)** Difference between the N/C ratio before and after the administration of the EMF (average of three experiments). The EMF (incident power: 5 W; exposure time: 10 s) was applied at 12 min. CNT: Carbon nanotube; Dox: Doxorubicin; N/C: Nuclear/cytoplasmic.

0.1°C). The EMF induced an increase of temperature, which exhibited a linear relation with the power used (R_2 = 0.0997). Following the application of the EMF, temperature values reached 31.4(±0.6)°C and 34.1(±0.6)°C for 10 and 20 s of exposure, respectively. Membrane breakdown due to thermal shock is unlikely to occur since this requires exposure of cells to temperatures >40°C for at least tens of seconds [42]. The temperature increase should arise from the absorption of water at these wavelengths rather than nanotubes. In order to confirm this assumption, we increased the nanotube concentration up to 60-fold, and the corresponding temperature increase was not statistically different from that achieved with pure water (data not shown). According to this finding, viability of cells exposed to the EMF did not vary significantly from the control cells (colony assay, see Supplementary Information 3).

Modeling the power transmission within the brain

We evaluated the exposure limit that cannot be exceeded in living animals in order to comply with existing guidelines. There are several published reports on the biological effects of EMF on human tissues [43]. Some of these concern tissue heating due to RF energy absorption, whereas others address possible carcinogenic effects. The IEEE C95.1–2005 "Standard for safety levels with respect to human exposure to radio frequency EMF, 3 kHz to 300 GHz" was issued to protect against established adverse effects in humans from exposure to RF. Specifically, in the frequency range of 100 kHz to 300 GHz, the guidelines protect against adverse health effects associated with heating. The frequency 100 kHz nominally represents a 'thermal crossover' below which electrostimulation effects dominate, and above which thermal effects dominate on continued wave exposure. Based on IEEE C95.1–2005 for upper tier, the maximum permissible exposures to a 10 GHz EMF for mice with a surface of 36 cm^2 should be 0.36 W for 100 s, corresponding to the energy dose of 36 J. Hence, we considered this limit during exposure of mice to EMF exposure in the *in vivo* experiments.

The system used to irradiate the mice consisted of a wave guide shaped like a little horn (see Supplementary Information 2). We used a HFSS tool to model the electric field distribution in the horn as a function of the power applied. The working frequency was set at 10 GHz and the input power from 1 to 14 W. The value of the power and the electric field at the end of the horn for different input power is provided in Table 1. Based on these data, we concluded that by applying an incident power of 5 W, the power at the end of the horn is 1.38 W: in order to satisfy the requirement of energy dose <36 J, the exposure time should be maintained below 25 s.

To determine whether this EMF (10 GHz,

3 cm wavelength, 5 W of incident power) can penetrate into the mouse brain and to what extent, we used HFSS analysis to model the penetration of the EMF inside the mouse brain. The mouse head was placed at the end of the horn. This simulation showed that the waves penetrate the cranial bones of the mouse and concentrate in the region corresponding to the chosen area treated by vector injection, where the electric field equated to 9000–10000 V m^{-1} for an incident power of 5 W.

In the case of a conductor wire (1 µm in length) exposed to this electrical field, the corresponding voltage induced at the antenna terminals approximated to 100 mV, which should be sufficient to alter the natural transmembrane potential of CNS cells (typically -70 mV). As a result of this, the membrane could become transiently permeabilized and normally impermeant molecules could enter the cell. The mechanism underlying this phenomenon could be similar to that proposed for cell electroporation (also called permeabilization). Electropermeabilization or electroporation (EP; i.e., the application of controlled electric fields to facilitate cell permeabilization) is an established technique for introducing molecules inside cells. Originally reported by Neumann *et al.* [44], it is nowadays used routinely for *in vitro* laboratory transfection experiments. Recent studies have shown that EP can be used to deliver genes efficiently *in vivo* to various tissues, including the CNS [45], and targeted electrochemotherapy for skin and subcutaneous cancers is well established in clinical practice [46]. While the exact mechanism of this long-lived transmembrane exchange is still unknown, a hypothesis originally proposed by Abidor *et al.* postulates that the formation of conductive pores in the lipid bilayer of the membrane exposed to a large transmembrane potential provides pathways for molecular transport [47]. The macromolecules then enter the cell through these cell membrane transient pores, either through electrophoresis in the case of charged molecules [48], or by passive diffusion in the case of neutral molecules [49]. Electroporation usually requires high voltages that can cause significant cell death [50]. In this context, the proposed methodology could offer an alternative approach to enhance the natural

Table 1. Values of power and electric field at the end of the horn for different input power.

Input power	Output power	Electric field
1 W	0.276 W	1508 V/m
5 W	1.38 W	3372 V/m
10 W	2.76 W	4770 V/m
14 W	3.86 W	5643 V/m

Frequency: 10 GHz.

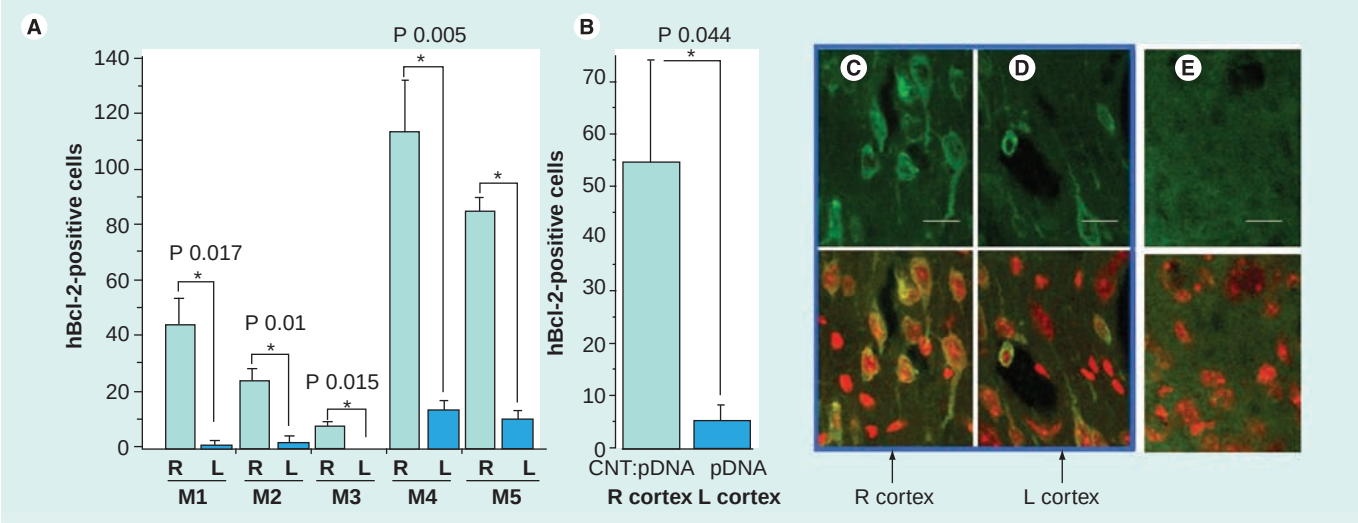

Figure 5. Expression of ectopic *hBcl-2* in cortical neurons. (A) Five mice (M1 to M5) were injected in the right hemisphere (R) with CNTs:pDNA and in the left hemisphere (L) with pDNA alone and irradiated for 20 s with a power of 5 W. The bar graph represents the average of hBcl-2 positive cells from three microscope fields selected adjacent to the injection site. **(B)** Average data. **(C)** Immune histochemistry of the coronal section through the cortex injected with CNTs:pDNA of an animal exposed to the EMF. **(D)** Immune histochemistry of coronal section through the cortex injected with pDNA of the same animal exposed to the EMF. **(E)** Immune histochemistry of section through the cortex injected with CNTs:pDNA of an animal exposed to a null EMF. The sections were treated with anti-Bcl-2 antibodies (green) and propidium iodide (PI, red). Top images: green stain for Bcl-2 alone. Bottom images: co-staining for Bcl-2 and PI. Scale bar 25 µm. *$p \leq 0.05$.
CNT: Carbon nanotube.

cell permeability. CNTs could work as nanotools able to alter the cell trasmembrane potential, allowing macromolules to enter within the cells. Concerning the fate of the nanotubes, we can speculate that they are unlikely to enter cells due to the difference of dimensions between the nanotubes (length 1 ± 0.5 µm) and pores (estimated to be in the range of 10–30 nm) [51].

In vivo experiments

The anaesthetized animals were exposed to the appropriate EMF using a dedicated source and external antenna for 20 s at an incident power of 5 W (n = 5), and to a null EMF (n = 5). All animals were then allowed to recover before sacrifice 48 h later with a harvest of brains for serial histological studies. Coronal sections through the cortex were probed with human selective Bcl-2 antibody. To avoid any possible cross reaction of the human antibody with the mouse endogenous Bcl-2 protein, we performed control experiments to confirm that the injection *per se* does not induce expression of *Bcl-2* in the motor cortex.

In the right hemisphere, injected with MWCNT:pDNA suspension, of mice exposed to EMF, the expression of the ectopic DNA was confirmed in several cells of the motor cortex by confocal microscopy (Figure 4). In controls (left hemisphere, injected with pDNA suspension, of mice exposed to EMF), *hBcl-2* expression was low to negligible. Similarly, no expression was observed in mice injected with MWCNT:pDNA and exposed to null EMF.

As shown in Figure 5A, the brain of each irradiated animal exhibited a significantly higher number of cells expressing the *hBcl-2* in proximity of the injected region with CNT:pDNA compared with the number of cells present in the left hemisphere injected with pDNA alone. However, the experiments revealed considerable variation in the level of transfection within the group of animals (Figure 5B). This variability can be explained by FEM analysis, which indicates that millimeter variation in distance and position of the animal from the source of the irradiation dramatically changes the amount of energy absorbed by CNT, and consequently the efficacy of transfection. These data established the proof-of-concept that the antenna proprieties of MWCNTs irradiated with the appropriate EMF can be safely and effectively applied to significantly enhance cell permeabilization in the CNS. We report here the successful uptake and expression of the *hBcl-2* transgenes *in vivo* (Figure 4).

Conclusion

This report describes, by a theoretical and experimental approach, the exploitation of the antenna properties of MWCNTs in cell lines and in live animals. The experiments confirmed that CNTs can induce noncontact cell membrane poration for drugs and genes to enter the cells when exposed to EMF in the microwave range. Most notably, we demonstrate that the CNT-mediated permeabilization can be successfully applied without causing damage to a complex system such as the brain. These observations point to future development of technologies for wireless electropermeabilization of tissues for targeting gene and drug therapy and to potential application in wireless electrostimulation for cardiac, neuromuscular and visceral myopathy disorders.

Executive summary

Multiwalled carbon nanotube-like antennas

- This study employed water solutions of singly dispersed multiwalled carbon nanotubes (MWCNTs) with a high degree of purity (97.06%) and low amorphous carbon (<1%).
- The nanotubes had diameters ranging from 19 to 40 nm and were 1 ± 0.5 µm in length.
- Finite element modeling based on the antenna theorem predicted that MWCNTs resemble thin-wire dipole antennas for electromagnetic wave propagation at or near the free-space velocity of light.
- CNT antennas have been employed to convert an electromagnetic radiation into energy current to facilitate cell permeabilization for enhanced cellular uptake of normally impermeable molecules.

In vitro *validation*

- CNT antenna-mediated cell permeabilization was validated in experiments involving immortalized fibroblast cell line (drug model: doxorubicin chemotherapeutic agent).
- The application of the EMF improved drug uptake and the phenomenon was strongly enhanced in the presence of CNTs.
- The combination of CNT and EMF treatment dramatically favored nuclear localization of the anticancer drug.

In vivo *validation*

- CNT antenna-mediated cell permeabilization was validated in living mice (drug model: Bcl-2 antiapoptotic gene) following stereotactic injection in the cerebral motor cortex of CNT:pDNA (right hemisphere) and pDNA (left hemisphere, control).
- FEM analysis showed that the EMF penetrates the cranial bones of the mouse and concentrate in the region corresponding to the injected area.
- The antenna properties of MWCNTs have been applied successfully to induce high level of gene expression locally into the mouse brain.

Acknowledgements

The authors would like to acknowledge L Mir from CNRS, Institute Gustave-Roussy, M Patè from Thales, PM Schmidt, M Bonazzi, C Gabellieri and M Cacace from EC and the other members of the NINIVE working team (i.e., G Ciofani from Scuola Superiore Sant'Anna [Italy], A Nunes from the School of Pharmacy of University of London [UK], and M Burghard, P Santhosh and N Amsharov from Max-Planck-Institut fuer Festkoerperforschung [Germany]).

Financial & competing interests disclosure

This work has been performed in the framework of the Non Invasive Nanotransducer for in vivo *gene therapy (NINIVE) project funded by the EC (contract number 033378). This work is also supported by MIUR (PRIN 2008). A Ziaei, V Raffa, O Vittorio, C Riggio, A Cuschieri, T Pizzorusso, M Costa, G Bardi, L Gherardini, KT Al-Jamal, S Nitodas and T Karachalios are awaiting a patent related to the content of this article. The authors have no other relevant affiliations or financial involvement with any organization or entity with a financial interest in or financial conflict with the subject matter or materials discussed in the manuscript apart from those disclosed.*

No writing assistance was utilized in the production of this manuscript.

References

Papers of special note have been highlighted as:
- ▪ of interest
- ▪▪ of considerable interest

1 Popov VN. Carbon nanotubes: properties and application. *Mater. Sci. Eng. R Rep.* 43, 61–102 (2004).

2 Tasis D, Tagmatarchis N, Bianco A, Prato M. Chemistry of carbon nanotubes. *Chem. Rev.* 106(3), 1105–1136 (2006).

3 Saito N, Usui Y, Aoki K *et al.* Carbon nanotubes: biomaterial applications. *Chem. Soc. Rev.* 38, 1897–1903 (2009).

4 Singh P. Carbon nanotube and their biomedical applications: a review. *Chalcogenide Lett.* 7, 389–396 (2010).

5 Johnston HJ, Hutchison GR, Christensen FM *et al.* A critical review of the biological mechanisms underlying the *in vivo* and *in vitro* toxicity of carbon nanotubes: the contribution of physico-chemical characteristics. *Nanotoxicology* 4, 207–246 (2010).

6 Shvedova AA, Castranova V, Kisin ER *et al.* Exposure to carbon nanotube material: assessment of nanotube cytotoxicity using human keratinocyte cells. *J. Toxicol. Environ. Health A* 66, 1909–1926 (2003).

7 Pulskamp K, Diabate S, Krug HF. Carbon nanotubes show no sign of acute toxicity but induce intracellular reactive oxygen species in dependence on contaminants. *Toxicology Letters* 168, 58–74 (2007).

8 Poland CA, Duffin R, Kinloch I *et al.* Carbon nanotubes introduced into the abdominal cavity of mice show asbestos like pathogenicity in a pilot study. *Nat. Nanotechnol.* 3, 423–428 (2008).

9 Wörle-Knirsch JM, Pulskamp K, Krug HF. Oops they did it again! Carbon nanotubes hoax scientists in viability assays. *Nano Lett.* 6, 1261–1268 (2006).

10 Ali-Boucetta H, Al-Jamal KT, Kostarelos K. Cytotoxic assessment of carbon nanotube interaction with cell cultures. *Methods Mol. Biol.* 726, 299–312 (2011).

11 Vittorio O, Raffa V, Cuschieri A. Biocompatibility of multi-wall carbon nanotubes on human neuroblastoma cell line and effects of metal impurity and surface oxidation. *Nanomedicine* 5, 424–431 (2009).

▪ ***In vitro* experiments confirmed that our multiwalled carbon nanotubes (MWCNTs) did not affect cell viability.**

12 Bardi G, Vittorio O, Maffei M, Pizzorusso T, Costa M. Adipocytes differentiation in the presence of Pluronic F127–coated carbon nanotubes. *Nanomedicine* 5, 378–381 (2009).

13 Bardi G, Tognini P, Ciofani G, Raffa V, Costa M, Pizzorusso T. Pluronic-coated carbon nanotubes do not induce degeneration of cortical neurons *in vivo* and *in vitro*. *Nanomedicine* 5, 96–104 (2009).

▪ ***In vivo* assays suggested that our MWCNTs injected in the mouse cerebral cortex did not induce apoptosis of cortical neurons.**

14 Edwards SL, Werkmeister JA, Ramshaw JAM. Carbon nanotubes in scaffolds for tissue engineering. *Expert Rev. Med. Devices* 6, 499–507 (2009).

15 Cellot G, Cilia E, Cipollone S *et al.* Carbon nanotubes might improve neuronal performance by favouring electrical shortcuts. *Nat. Nanotechnol.* 4, 126–133 (2009).

16 Mazzatenta A, Giugliano M, Campidelli L *et al.* Interfacing neurons with carbon nanotubes: electrical signal transfer and synaptic stimulation in cultured brain circuits. *J. Neurosci.* 27, 6931–6936 (2007).

17 Malarkey EB, Fisher KA, Bekyarova E, Liu W, Haddon RC, Parpura V. Conductive single-walled carbon nanotube substrates modulate neuronal growth. *Nano Lett.* 9, 264–268 (2009).

18 Kotov NA, Winter JO, Clements IP *et al.* Nanomaterials for neural interfaces. *Adv. Mater.* 21, 3970–4004 (2009).

19 Malarkey EB, Parpura V. Carbon nanotubes in neuroscience. *Acta Neurochir. Suppl.* 106, 337–341 (2010).

20 Raffa V, Ciofani C, Vittorio O, Riggio C, Cuschieri A. Physicochemical properties affecting cellular uptake of carbon nanotubes. *Nanomedicine (Lond.)* 5(1), 89–97 (2010).

21 Lacerda L, Raffa V, Prato M, Bianco A, Kostarelos K. Cell-penetrating carbon nanotubes in the delivery of therapeutics. *Nano Today* 2(6), 38–43 (2007).

22 Kostarelos K, Bianco A, Prato M. Promises, facts and challenges for carbon nanotubes in imaging and therapeutics. *Nat. Nanotechnol.* 4, 627–633 (2009).

23 Prato M, Kostarelos K, Bianco A. Functionalized carbon nanotubes in drug design and discovery. *Acc. Chem. Res.* 41, 60–68 (2008).

24 Foldvari M, Bagonluri M. Carbon nanotubes as functional excipients for nanomedicines: II. drug delivery and biocompatibility issues. *Nanomedicine* 4, 183–200 (2008).

25 Foldvari M, Bagonluri M. Carbon nanotubes as functional excipients for nanomedicines: I. pharmaceutical properties. *Nanomedicine NBM* 4, 173–182 (2008).

26 Raffa V, Ciofani G, Nitodas S, Karachalios T, D'Alessandro D, Masini M. Can the properties of carbon nanotubes influence their internalisation by living cells? *Carbon* 46, 1600–1610 (2008).

27 Shi Kam W, O'Connell M, Wisdom JA, Dai H. Carbon nanotubes as multifunctional biological transporters and near-infrared agents for selective cancer cell destruction. *Proc. Natl Acad. Sci. USA* 102, 11600–11605 (2005).

28 Gannon CJ, Cherukuri P, Yakobson BI *et al.* Carbon nanotube-enhanced thermal destruction of cancer cells in a noninvasive radiofrequency field. *Cancer* 110(12), 2654–2665 (2007).

- **Single-walled carbon nanotubes have been shown to efficiently convert electromagnetic radiation into heat across radiofrequency and this has been exploited for thermal ablation of malignant cells.**

29 Rojas-Chapana JA, Correa-Duarte MA, Ren Z, Kempa K, Giersig M. Enhanced introduction of gold nanoparticles into vital acidothiobacillus ferrooxidans by carbon nanotube-based microwave electroporation. *Nano Lett.* 4, 985–988 (2004).

- **The authors propose a method that exploits the field emission properties of MWCNTs to electroporate Gram-negative bacteria.**

30 Raffa V, Ciofani G, Vittorio O, Pensabene V, Cuschieri A. Carbon nanotube-enhanced cell electropermeabilisation. *Bioelectrochemistry* 79(1), 136–141 (2010).

- **The authors propose a method that exploits the dielectric properties of MWCNTs to facilitate cell permeabilization for enhanced cellular uptake of small molecules.**

31 Pensabene V, Vittorio O, Raffa V, Ziaei A, Menciassi A, Dario P. Neuroblastoma cells displacement by magnetic carbon nanotubes. *IEEE Trans. Nanobioscience* 7(2), 105–110 (2008).

32 Ciofani G, Raffa V, Pensabene V, Menciassi A, Dario P. Dispersion of multiwall carbon nanotubes in aqueous Pluronic F127 solutions for biological applications. *Full. Nano. Carbon Nanostruct.* 17, 11–25 (2009).

33 Chierzi S, Cenni MC, Maffei L *et al.* Protection or retinal ganglion cells and preservation of function after optic nerve lesion in bcl-2 transgenic mice. *Vision Res.* 38, 1537–1543 (1998).

34 Jin YL, Chen JY, Xu L, Wang PN. Refractive index measurement for biomaterial samples by total internal reflection. *Phys. Med. Biol.* 51, N371–N379 (2006).

35 Romer AS, Parsons TTS. In: *The Vertebrate Body*. Holt-Saunders International, PA, USA 461–462 (1977).

36 Gabriel S, Lau RW, Gabriel C. The dielectric properties of biological tissues: II. Measurements in the frequency range 10 Hz to 20 GHz. *Phys. Med. Biol.* 41(11), 2251–2269 (1996).

37 Elwi TA, Al-Rizzo HM, Rucker DG, Dervishi E, Li ZR, Biris AS. Multi-walled carbon nanotube-based RF antennas. *Nanotechnology* 21(4), 045301 (2010).

- **Recently, Elwi and colleagues showed that antennas fabricated from networks of MWCNTs resonate in the microwave frequency range.**

38 Marchi M, Guarda A, Bergo A *et al.* Spatio-temporal dynamics and localization of MeCP2 and pathological mutants in living cells. *Epigenetics* 2, 187–197 (2007).

39 Costa M, Marchi M, Cardarelli F *et al.* Dynamic regulation of ERK2 nuclear translocation and mobility in living cells. *J. Cell Sci.* 119, 4952–4963 (2006).

40 Caleo M, Cenni MC, Costa M *et al.* Expression of BCL-2 via adeno-associated virus vectors rescues thalamic neurons after visual cortex lesion in the adult rat. *Eur. J. Neurosci.* 15, 1271–1277 (2002).

41 Dalmark M, Storm HH. A Fickian diffusion transport process with features of transport catalysis. Doxorubicin transport in human red blood cells. *J. Gen. Physiol.* 78(4), 349–364 (1981).

42 Tsong TY, Su ZD. Biological effects of electric shock and heat denaturation and oxidation of molecules, membranes, and cellular functions. *Ann. NY Acad. Sci.* 888, 211–232 (1999).

43 Polk C, Postow E. *Handbook of biological effects of electromagnetic fields*. CRC Press (1996).

44 Neumann E, Kakorin S, Toensing K. Fundamentals of electroporative delivery of drugs and genes. *Bioelectrochem. Bioenerg.* 48, 3–16 (1999).

45 De Vry J, Martínez-Martínez P, Losen M *et al. In vivo* electroporation of the central nervous system: a non-viral approach for targeted gene delivery. *Prog. Neurobiol.* 92, 227–244 (2010).

46 Heller LC, Heller R. *In vivo* electroporation for gene therapy. *Hum. Gene Ther.* 17, 890–897 (2006).

47 Abidor IG, Arakelyan VB, Chernomordik LV, Chizmadzhev YA, Pastushenko VF, Tarasevich MR. Electric breakdown of bilayer lipid membranes: I. Main experimental facts and their qualitative discussion. *Bioelectrochem. Bioenerg.* 6, 37–52 (1979).

48 Neumann E, Kakorin S, Tsoneva I, Nikolova B, Tomov T. Calcium-mediated DNA adsorption to yeast cells and kinetics of cell transformation by electroporation. *Biophys. J.* 71, 868–877 (1996).

49 Neumann E, Tonsing K, Kakorin S, Budde P, Frey J. Mechanism of electroporative dye uptake by mouse B cells. *Biophys. J.* 74, 98–108 (1998).

50 Meaking WS, Edgerton J, Wharton CW, Meldrum RA. Electroporation-induced damage in mammalian cell DNA. *Biochim. Biophys. Acta* 1264, 357–362 (1995).

51 Krassowska W, Filev PD. Modeling electroporation in a single cell. *Biophys. J.* 92, 404–417 (2007).